Neuroscience Letters 664 (2018) 160–166

Contents lists available at ScienceDirect

Neuroscience Letters

journal homepage: www.elsevier.com/locate/neulet

Research article

Region-specific alterations in astrocyte and microglia morphology following exposure to blasts in the mouse hippocampus

Gloria J. DeWalt*, Biraaj Mahajan, Andrea R. Foster, Lauren D.E. Thompson, Andrew A. Marttini, Eric V. Schmidt, Sara Mansuri, Dwayne D'Souza, Shama B. Patel, Madeline Tenenbaum, Karla I. Brandao-Viruet, Dominique Thompson, Bryan Duong, Danica H. Smith, Todd A. Blute, William D. Eldred

Boston University, Department of Biology, United States

GRAPHICAL ABSTRACT

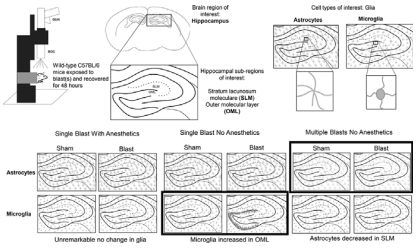

ARTICLE INFO

Keywords:
Stratum lacunosm moleculare
Outer molecular layer
Glia
Blast injury
Ketamine/xylazine

ABSTRACT

Traumatic brain injury (TBI) is a serious public health concern, especially injuries from repetitive insults. The main objective of this study was to immunocytochemically examine morphological alterations in astrocytes and microglia in the hippocampus 48 h following a single blast versus multiple blasts in adult C57BL/6 mice. The effects of ketamine and xylazine (KX), two common anesthetic agents used in TBI research, were also evaluated due to the confounding effect of anesthetics on injury outcome. Results showed a significant increase in hypertrophic microglia that was limited to the outer molecular layer of the dentate gyrus, but only in the absence of KX. Although the presence or absence of KX had no effect on astrocytes following a single blast, a significant decrease in astrocytic immunoreactivity was observed in the stratum lacunosum moleculare following multiple blasts in the absence of KX. The morphological changes in astrocytes and microglia reported in this study reveal region-specific differences in the absence of KX that could have significant implications for our interpretation of glial alterations in animal models of injury.

1. Introduction

Traumatic brain injury (TBI) is one of the leading causes of death and disability in developed nations [1]. In particular, TBI from blasts in military settings are so prevalent, it is known as the 'signature' wound of warfare [1–3]. Injuries from blast are categorized as: primary (pathology from the actual blast wave), secondary (damage from penetrating fragments), tertiary (injury due to displacement into

Abbreviations: AD, Alzheimer's disease; COBIA, cranium only blast injury apparatus; GFAP, glial fibrillary acidic protein; Iba1, ionized calcium binding adapter molecule 1; kPa, kilopascal; KX, ketamine/xylazine; OML, outer molecular layer; SD, Standard deviation; SLM, stratum lacunosm moleculare; TB, Itraumatic brain injury; ROI, region of interest

* Corresponding author.
E-mail address: dewaltg@bu.edu (G.J. DeWalt).

https://doi.org/10.1016/j.neulet.2017.11.016
Received 31 July 2017; Received in revised form 7 November 2017; Accepted 7 November 2017
Available online 11 November 2017
0304-3940/

surrounding structures) and quaternary (insult from burns and noxious fumes), yet primary injury represents a unique and prevalent mode of pathology [4,5]. Although moderate and severe insults receive considerable attention, mild TBI accounts for the majority of injuries [6].

Subtle cellular pathologies, evident only on a microscopic level, may be critical to the progression of injury [7]. Astrocytes and microglia are glial cells sensitive to changes in the microenvironment, particularly following injury [8,9]. A remarkable feature of both is their ability to reversibly assume different morphologies. In healthy tissue, microglia are dynamic sentinels that extend and retract thin ramified processes to survey the microenvironment and interact with nearby cells. Microglial morphologies range from hypertrophied somata and processes to complete contraction of processes when fully activated resulting in an amoeboid-like appearance [10,11]. Similarly, astrocytes can undergo morphological changes following insult [12,13]. Hypertrophy of astrocytes and microglia can occur rapidly (minutes to hours) and persist (weeks to years) following insult [14]. In this study, we used immunocytochemistry to evaluate morphological changes in astrocytes and microglia in different hippocampal sub-regions due to previous reports citing hippocampal deficits in learning and memory following TBI [15–17].

Anesthetics and analgesics are routinely used in many animal models of TBI based due to ethical considerations to minimize pain and distress whenever possible. However, compelling evidence has shown that anesthetics can affect injury progression [18,19]. It is believed that anesthetics and analgesics are neuroprotective via anti-excitotoxic and anti-apoptotic actions [19,20], although there are some studies that have reported exacerbation of injury outcome [18]. A consensus regarding the effect of various anesthetics and analgesics on glia has yet to be reached, as protective or detrimental outcomes are influenced by age and mode of injury [21,22]. Therefore, in the first experiment, our goal was to document whether the presence of ketamine and xylazine (KX), a commonly used anesthetic/analgesic combination, would affect glia acutely following exposure to a single blast. It has become increasingly evident that studies incorporating exposure to multiple blasts can offer insight into TBI pathology, as TBI injuries are often due to repetitive insults [23,24]. Thus, in the second part of this study, we examined differences in glial morphologies using a repetitive blast paradigm without KX.

2. Methods

2.1. Blast apparatus

Blast overpressures were generated using a previously characterized cranium only blast injury apparatus (COBIA) [25]. The main component of the apparatus was a modified 0.22 caliber, single-shot, powder-actuated tool (Ramset RS22; ITW Ramset, Glendale Heights, IL). The piston that normally drives the fastener was removed causing it to function as a small blast tube. The tool was mounted vertically using a custom-fabricated stand that allowed consistent positioning. Blasts were directed downward through a blast director (Fig. 1A) fabricated from polyvinyl chloride piping. The blast wave was generated by firing a 0.22 caliber blank cartridge (Ramset power level 4). A high frequency piezoelectric pressure transducer (Model: 113B21 High Frequency ICP® pressure sensor, PCB Piezotronics, Inc., Depew, New York) was used to measure the pressure produced. Calibrations were carried out with the sensor positioned where the head of the mouse would be during the blast procedure. A constant current power supply (Model 5421, Columbia Research Laboratories, Inc., Woodlyn, PA) provided power to the sensor. Outputs were digitized with an analog to digital converter (Analog Devices, ADAS3022) and saved as waveforms for offline analysis. The average blast pressure was 1034 kPa (n = 10, SD = 220).

2.2. Blast procedure

All blast protocols were approved by the Boston University Institutional Animal Care and Use Committee. Wild-type C57BL/6 mice (2–6 months, Charles River Laboratories) were kept on 12 h: 12 h light-dark cycle with free access to food and water. Sham mice were treated exactly the same, with the exception of exposure to blast.

An intraperitoneal injection of KX (75 mg/kg, ketamine; 13 mg/kg, xylazine) was administered at least 10 min prior to each blast procedure. Anesthetized animals (sham = 5, blast = 7) were placed in a prone position within a cylindrical mouse restrainer (Stoelting Co. Wood Dale, IL) with the dorsal surface of the head positioned two centimeters under the opening of the blast director. Blasts were directed between bregma and lambda. To prevent potential quaternary damage from gun powder during blasts a wetted paper cone was placed over the head. The wetted cone provided reproducible positioning while still allowing maximal downward free acceleration of the head from the primary blast. Unanesthetized mice (sham = 5; blast = 6) were similarly handled and positioned.

The triple blast paradigm, conducted in the absence of KX (sham = 3; blast = 5), occurred daily for three consecutive days. The 24 h latency between each blast was based on a previously published focal model of TBI that showed exacerbated pathologies when multiple insults occurred 24 h apart [26]. Fig. 1B, diagrams the single versus triple blast paradigms.

Formal behavioral assessments to quantitatively probe the nuances of functional impairments were not conducted. However, careful observation of the mice following the blast procedures did not reveal overt defects in gait, grooming, or feeding. None of the blasted mice lost consciousness. Furthermore, there were no signs of contusions or gross tissue damage in the blasted brains, or in sections of the brains during postmortem examination. Although 1034 kPa represents a high peak overpressure, due to its short duration and absence of lethality, the nature of insult(s) experienced by the animals in this study were not considered severe.

2.3. Tissue preparation

Forty-eight hours after the final blast the mice were deeply anesthetized with isofluorane and then transcardially perfused with 0.9% heparinized saline followed by 4% paraformaldehyde in 0.1 M phosphate buffer (PB, pH 7.4). Immediately following perfusion, brains were removed intact, immersed in 4% paraformaldehyde in PB, and post-fixed overnight at 4° C. Following immersion fixation, brains were rinsed in PB and cryoprotected in a graded sucrose series in PB (5–30%). Serial 40 μm coronal sections were cut using a freezing stage sliding microtome. Slices were stored in an antifreeze solution (30% sucrose, 30% ethylene glycol, 1% polyvinylpyrrolidone in Tris-buffered saline (pH 7.6) for long term storage at −20° C.

2.4. Immunocytochemistry

Three slices from each animal sampled between bregma −1.46 to −3.28 mm [27] were washed in several changes of PB on a rotator to completely remove residual cryoprotectant, mounted onto Colorfrost Plus slides (ThermoFisher Scientific, Waltham, MA), and allowed to air-dry for one hour. Sections were rehydrated in PB and blocked in 5% normal donkey serum (Jackson Immuno Research Laboratory, Inc. West Grove, PA) diluted in PB with 0.3% Triton X-100 (PBTx) for one hour at room temperature. Slices were incubated overnight at 4° C in either a mouse monoclonal antisera directed against glial fibrillary acidic protein (GFAP), an intermediate filament protein within mature astrocytes that is responsible for changes in morphology and movement [28,29] (GFAP 1:100, Clone No. N206 A/8, UC Davis/NIH NeuroMab Facility Cat# 75–240, RRID:AB_10672299) or a polyclonal rabbit antisera directed against ionized calcium binding adapter molecule 1 (Iba1), a

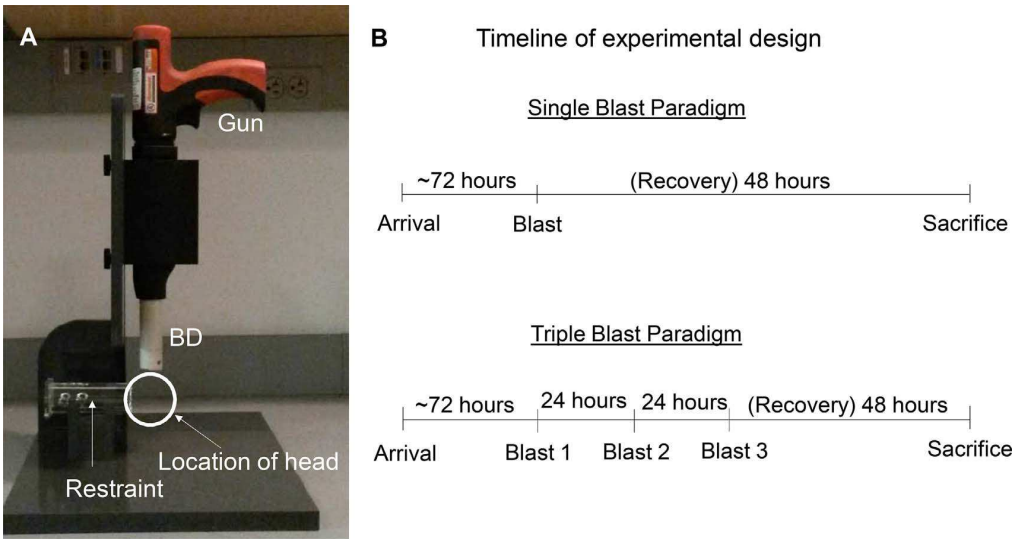

Fig. 1. Experimental design. (A) The Cranium Only Blast Injury Apparatus (COBIA) used to simulate primary blast. BD = blast director. (B) Timeline of single versus triple blast paradigms.

calcium binding protein found in microglia (1:500, Wako, Catalog No. 019-19741, RRID:AB_839504).

Following incubation in primary, the slides were washed in PB and the appropriate secondary antiserum was applied (donkey anti-mouse Cy-3 or donkey anti-rabbit 647; Jackson Immuno Research diluted 1:500 in PBTx) for two hours at room temperature. Following several washes in PB, sections were coverslipped using Vectashield with DAPI (Vector Labs, Burlingame, CA). Some slices were processed without primary antisera and exhibited no immunoreactivity. Both of these antisera have been previously characterized in mice [30,31].

2.5. Imaging

A Nikon Eclipse microscope with Elements AR software (Nikon Instruments, Inc.) was used to image sections at 10x. Illumination and acquisition settings were matched across each animal. ImageJ software (Rasband, W.S., ImageJ, U. S. National Institutes of Health, Bethesda, Maryland, USA, https://imagej.nih.gov/ij/, 1997–2016) was used to analyze immunostaining. The display range for all images were matched and then inverted so that signal appeared black.

2.6. Evaluation of GFAP positive astrocytes and Iba1 positive microglia

All analyses were performed on coded sections by an observer blinded to conditions.

2.6.1. GFAP

GFAP immunoreactivity in the stratum lacunosm moleculare (SLM) was compared between sham and blast exposed animals because it showed the strongest immunoreactivity. However, GFAP positive astrocytes surrounding vasculature within the SLM hindered unambiguous identification of individual astrocytes. Therefore, we analyzed the percent area occupied by GFAP immunoreactivity in the SLM. We hypothesized that hypertrophy would be reflected in a greater percent area. Inverted grayscale images were first binarized using the isodata thresholding algorithm in ImageJ. A region of interest (ROI) large enough to encompass the SLM in each section was created and applied to each hemisphere (Fig. 2A). The percent area of GFAP immunoreactivity within each ROI was obtained for each image using the area fraction selection from the ImageJ measure plugin (Fig. 2, A1-3). Measurements were obtained for each ROI, averaged by animal, and then by condition.

2.6.2. Iba1

The outer molecular layer (OML) of the dentate gyrus (Fig. 2B) was selected for evaluation due to the concentration of hypertrophic phenotypes in this sub-region. An ROI, large enough to encompass the OML, was created and applied to the OML in each hemisphere (Fig. 2, B1-2). Two broad classifications of microglial phenotypes were chosen for evaluation: ramified and hypertrophic [11]. Manual counts of ramified versus hypertrophic phenotypes were obtained from Iba1 positive cells with clearly labeled somata (Fig. 2B1-2).

2.7. Statistics

SPSS (IBM Corp. Released 2016. IBM SPSS Statistics for Windows, Version 24.0. Armonk, NY: IBM Corp.) was used for statistical analyses. A one-way analysis of variance (ANOVA) was used to determine whether there were significant differences in the percent area occupied by GFAP or counts of Iba1 positive hypertrophy in sham versus blast exposed mice. The Welch's test was used when violations to the homogeneity of variance occurred. A Bonferroni *post hoc* correction was used for multiple comparisons when significant differences were observed (alpha < 0.05). Analyses were first conducted to explore whether the presence of KX had a significant effect on astrocytes and microglia following a single blast (Experiment 1). Subsequent analyses to compare differences following a single or triple blast were performed in the absence of KX (Experiment 2) to avoid any confounding effects from KX. No significant differences were found in the presence or absence of KX between the sham cohorts ($p = 0.102$; single 48 h $n = 5$, triple 48 h $n = 3$), therefore the data from both sham cohorts were pooled and compared to each blast group (single versus triple blast). Graphs are presented as mean ± SD.

3. Results

3.1. Experiment 1: the effect of KX on GFAP and Iba1 immunoreactivity after a single blast

In the presence of KX, there was no significant difference ($p = 0.515$) in the average number of hypertrophic microglia in the OML between sham and blast groups (Fig. 3A). However, in the absence

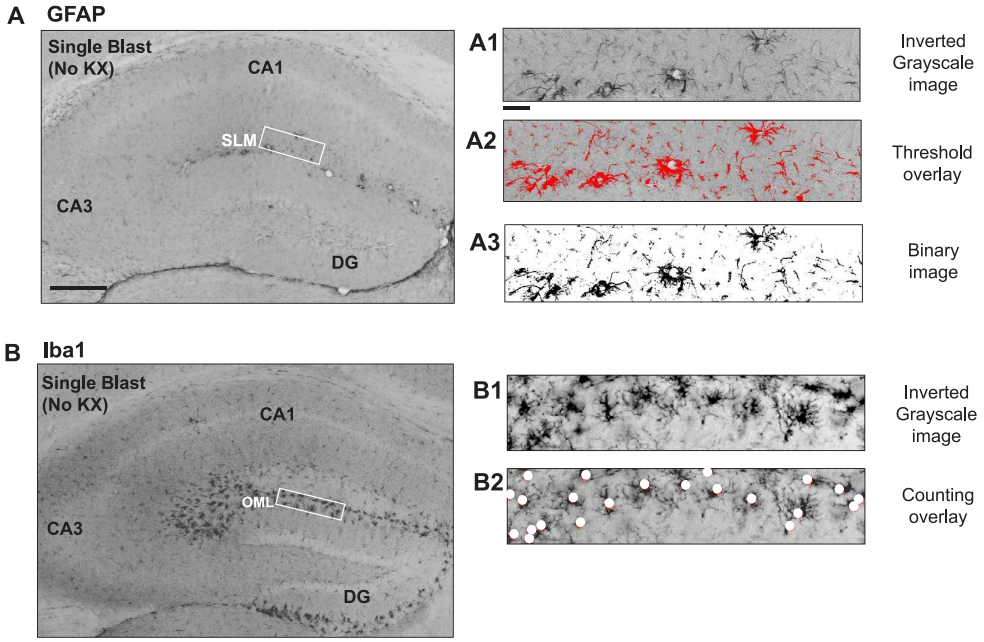

Fig. 2. Evaluation of immunostaining. (A) GFAP immunostaining following a single blast without KX. Zoom of ROI analyzed (A1). Example threshold overlay (A2) and the resulting binary image (A3). CA1 = cornu ammonis 1. CA3 = cornu ammonis 3. DG = dentate gyrus. ROI = region of interest. SLM = stratum lacunosum moleculare. (B) Iba1 immunostaining following a single blast without KX. Zoom of ROI analyzed (B1) and resulting manual counts (B2). OML = outer molecular layer. ROI = region of interest. Scale bars = 250 μm (A and B); 20 μm (A1-3 and B1-2).

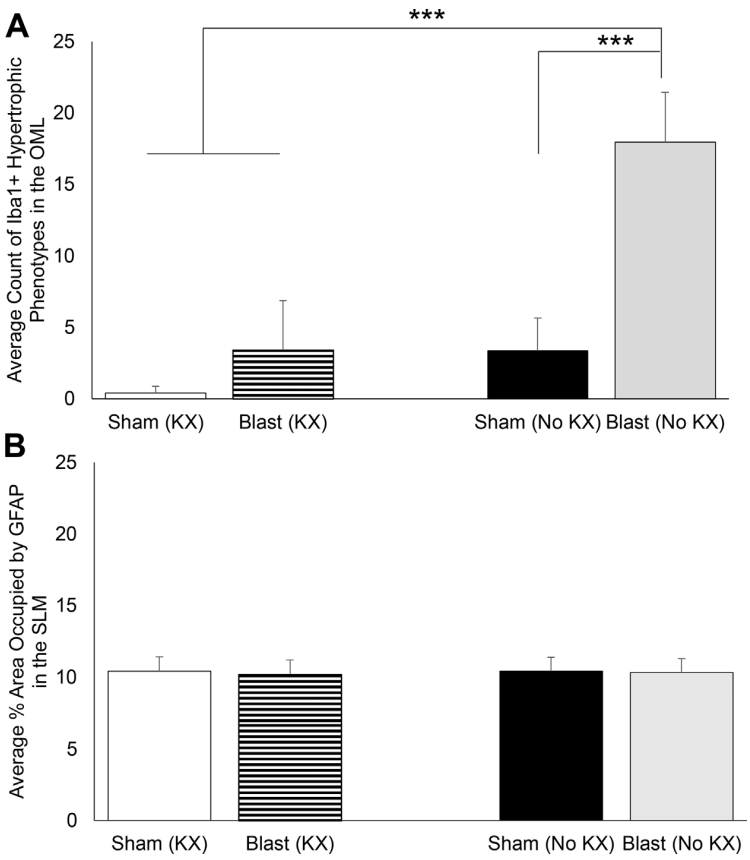

Fig. 3. The effect of KX on Iba1 positive microglia and GFAP positive astrocytes following a single blast. (A) In the absence of KX there were significantly more ($p < 0.001$) hypertrophic Iba1 positive cells in the outer molecular layer (OML) of the dentate gyrus in blast exposed animals compared to sham and blast exposed animals that received KX. (B) No differences were observed in the average percent area occupied by GFAP in the stratum lacunosum (SLM) in the presence or absence of KX. Sham (KX) = 5; Blast (KX) = 7; Sham (No KX) = 5; Blast (No KX) = 6. Error bars represent SD.

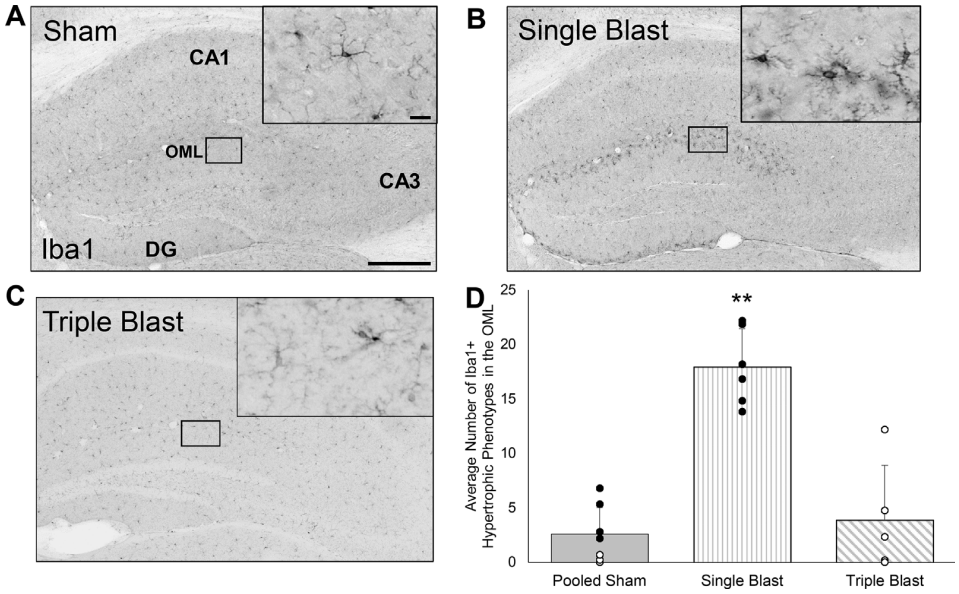

Fig. 4. Hypertrophic microglia were restricted to the outer molecular layer of the dentate gyrus after a single blast in the absence of KX. (A) Representative sham shows ramified Iba1 positive cells with thin processes (inset). CA1 = cornu ammonis 1. CA3 = cornu ammonis 3. DG = dentate gyrus. OML = outer molecular layer. Scale bar = 250 μm (inset 15 μm). (B) Following a single blast hypertrophic microglia were limited to the OML. Inset shows examples of hypertrophic Iba1 positive microglia. (C) In the triple blast paradigm there were few hypertrophic microglia. (D) Significantly more hypertrophic Iba1 ($p < 0.05$) were present in the OML after a single blast relative to triple blast and pooled shams (filled circles represent sham mice from the single blast paradigm, open indicate sham animals from the triple blast paradigm). Error bars represent SD.

of KX, there was a significant increase in hypertrophic cells ($F(3.19) = 44.808$, $p < 0.001$) present in blast exposed animals relative to sham (Fig. 3A). The percent area occupied by GFAP in the SLM (Fig. 3B) was not altered following blast in the presence or absence of KX ($p = 0.757$).

3.2. Experiment 2: the effect of multiple blasts on GFAP and Iba1 immunoreactivity in the absence of KX

Due to the previous confound produced by KX, this experiment was conducted without KX. Microglia were evaluated in sham animals as well as blast exposed mice following exposure to a single or triple blast (Fig. 4A–C). Iba1 positive microglia were classified as ramified or hypertrophic based on previously established morphological phenotypes [32]. No amoeboid morphologies were observed. Significantly more hypertrophic cells ($F(2.14) = 25.946$, $p < 0.001$) were present in the OML following a single blast relative to triple blast and pooled sham (Fig. 4D).

There was no difference ($p = 1.000$) in the percent area occupied by GFAP in the SLM in mice exposed to a single blast relative to sham (Fig. 5). However, following three blasts, there was a significant reduction ($F(2.16) = 7.083$, $p = 0.006$) in the average percent area of GFAP immunoreactivity (Fig. 5D).

4. Discussion

4.1. The presence of KX affects glial morphology in response to blast

Results of this study provide evidence that the presence of KX, a commonly used anesthetic/analgesic combination, can confound injury outcome acutely following primary blast insults. The average number of hypertrophic microglia were markedly increased in the absence of KX. Interestingly, the percent area occupied by astrocytes remained unchanged following blasts in animals with and without KX. This suggests that at the time point examined, microglia were more responsive to blast insults than astrocytes.

Because different TBI models are used to simulate specific forms of clinically relevant injuries, we need to understand the effect of anesthetics and analgesics. The confounding effects that various anesthetic and analgesic combinations can cause must be taken into account when interpreting results, particularly following less severe insults. Although isoflurane is often used in some TBI models [18,19], we did not evaluate its effect in our study because its administration would have prohibited the necessary head movement following blasts in our model.

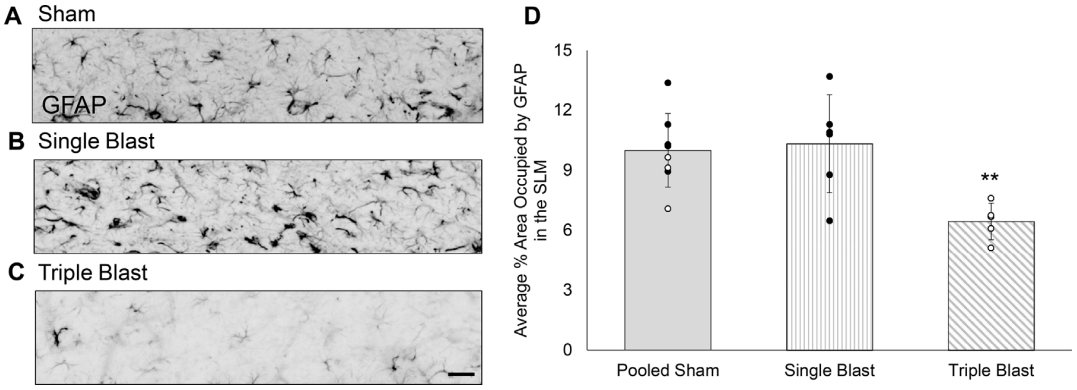

Fig. 5. GFAP immunoreactivity. (A-C) GFAP immunostaining in the stratum lacunosm moleculare (SLM). Scale bar = 20 μm. (B) The percent area occupied by GFAP in the SLM is significantly reduced following three blasts ($p < 0.01$) in comparison to a single blast and pooled shams (filled circles represent sham mice from the single blast paradigm, open indicate sham animals from the triple blast paradigm). Error bars represent SD.

Even if isoflurane was transiently administered and removed before blast to still allow free head movement, its residual effects could still confound results. However, a more detailed future study of the effects of isoflurane in our blast model is warranted.

4.2. Significant reduction of GFAP immunoreactivity in the SLM following multiple blasts in the absence of KX

The SLM, located within cornu ammonis 1 (CA1), receives direct projections from the entorhinal cortex [33] and contains a high density of blood vessels [34]. Microvasculature vulnerability in the cortex and hippocampus has been observed acutely (24 h) following consecutive blasts [24]. Astrocytes have a significant role in maintaining neuronal and vascular networks [35,36]. Therefore, it is reasonable that the integrity of the blood vessels or projections within this region may have been affected following blasts.

The decrease in the percent area occupied by GFAP immunoreactivity following triple blasts was initially unexpected. However, evidence of reduced GFAP immunoreactivity following injury has been reported previously and is attributed to the breakdown of intermediate filaments and a concomitant alteration in overall protein function [37]. Based on the diffuse nature of blast injury [38,39], it is possible that a similar mechanism could underlie the reduced GFAP we observed in the SLM.

4.3. Hypertrophic Iba1 restricted to the OML following exposure to a single blast in the absence of KX

The dentate gyrus receives cortical inputs to the hippocampus [40,41]. In particular, the molecular layer of the dentate gyrus is a highly laminated region with processes from granule cells throughout, as well as inputs from the entorhinal cortices in the OML [42,43]. Thus, it is possible that the hypertrophic microglia present in the OML could represent a regional sensitivity to blast. In particular, specific synaptic circuits and intricate interactions of microglia with adjacent neurons and glia in this region could affect the overall neuronal activity within this hippocampal sub-region.

Microglia are broadly classified as cytotoxic M1 (classical activation) or neuroprotective M2 (alternative activation/acquired deactivation) [44]. The identity of microglia (M1 vs. M2) is determined by secreted mediators, cell surface receptors, and alterations in gene expression. Future molecular or biochemical assays to identify changes in levels of relevant ions/neurotransmitters or gene expression, which are more sensitive than immunocytochemistry, could provide insight underlying the spatial hypertrophy we observed in the OML.

To our knowledge the only other study reporting pathology in the OML is a mouse model of Alzheimer's disease (AD) that showed amyloid beta pathology in the OML of transgenic mice [45]. However, no hypothesis to account for the regional pathology was provided. Due to reports [46,47] citing AD as a long term consequence of TBI, the similarity of the spatial specificity of the amyloid-beta pathology and the hypertrophic microglia we report is of great interest. It is possible that the hypertrophy observed in the OML represents a regional susceptibility in this paradigm. Based on microglial dynamics [10,11,14] and the lack of significant hypertrophy following multiple blasts, it is also possible that this region specific alteration is transient. It will be important for future studies to examine the impact of KX exposure on repeated blast injury induced glial responses in more detail. Future behavioral and molecular studies using this simple blast model will enable greater clarity into the nature/severity of the pathology, and provide insights into the clinical relevance of the timing of repeated injuries in order to identify mechanisms that underlie the glial changes observed.

Contributions

Manuscript composition, data analysis: GJD. Tissue processing: BM, ARF, LDET, AAM, EVS, SM, DD, SBP, MT, KIB, DT, BD, DHS. Guidance and study design: TAB, WDE.

Funding

Boston University Undergraduate Research Opportunities Programs to: ARF, LDET, EVS, DD, SBP, MT, KBV. HHMI to: ARF. Summer Undergraduate Research Fellowship Program (National Science Foundation) to: AAM, DT.

Acknowledgements

The authors thank Dr. Ian G. Davison and Ellen D. Witkowski for many of the animals used in this study and Dr. James A. Cherry for helpful feedback.

References

[1] K.R. Walker, G. Tesco, Molecular mechanisms of cognitive dysfunction following traumatic brain injury, Front. Aging Neurosci. 5 (2013) 29.
[2] A.K. Shetty, V. Mishra, M. Kodali, B. Hattiangady, Blood brain barrier dysfunction and delayed neurological deficits in mild traumatic brain injury induced by blast shock waves, Front. Cell. Neurosci. 8 (2014) 232.
[3] G.A. Elder, A. Cristian, Blast-related mild traumatic brain injury: mechanisms of injury and impact on clinical care, Mt. Sinai J. Med. 76 (2) (2009) 111–118.
[4] I. Cernak, L.J. Noble-Haeusslein, Traumatic brain injury: an overview of pathobiology with emphasis on military populations, J. Cereb. Blood Flow Metab. 30 (2) (2010) 255–266.
[5] I. Cernak, Animal models of head trauma, NeuroRx 2 (3) (2005) 410–422.
[6] C.P. Almeida-Suhett, E.M. Prager, V. Pidoplichko, T.H. Figueiredo, A.M. Marini, Z. Li, L.E. Eiden, M.F. Braga, GABAergic interneuronal loss and reduced inhibitory synaptic transmission in the hippocampal CA1 region after mild traumatic brain injury, Exp. Neurol. 273 (2015) 11–23.
[7] S. Patt, M. Brodhun, Neuropathological sequelae of traumatic injury in the brain. An overview, Exp. Toxicol. Pathol. 51 (2) (1999) 119–123.
[8] J.A. Goodrich, J.H. Kim, R. Situ, W. Taylor, T. Westmoreland, F. Du, S. Parks, G. Ling, J.Y. Hwang, A. Rapuano, F.A. Bandak, N.C. de Lanerolle, Neuronal and glial changes in the brain resulting from explosive blast in an experimental model, Acta Neuropathol. Commun. 4 (1) (2016) 124.
[9] N.C. de Lanerolle, F. Bandak, D. Kang, A.Y. Li, F. Du, P. Swauger, S. Parks, G. Ling, J.H. Kim, Characteristics of an explosive blast-induced brain injury in an experimental model, J. Neuropathol. Exp. Neurol. 70 (11) (2011) 1046–1057.
[10] M. Schwartz, O. Butovsky, W. Bruck, U.K. Hanisch, Microglial phenotype: is the commitment reversible? Trends Neurosci. 29 (2) (2006) 68–74.
[11] A. Karperien, H. Ahammer, H.F. Jelinek, Quantitating the subtleties of microglial morphology with fractal analysis, Front. Cell. Neurosci. 7 (2013) 3.
[12] J.D. Cherry, J.A. Olschowka, M.K. O'Banion, Neuroinflammation and M2 microglia: the good, the bad, and the inflamed, J. Neuroinflammation 11 (2014) 98.
[13] Y. Chen, R.A. Swanson, Astrocytes and brain injury, J. Cereb. Blood Flow Metab. 23 (2) (2003) 137–149.
[14] I.P. Karve, J.M. Taylor, P.J. Crack, The contribution of astrocytes and microglia to traumatic brain injury, Br. J. Pharmacol. 173 (4) (2016) 692–702.
[15] M. Beamer, S.R. Tummala, D. Gullotti, K. Kopil, S. Gorka, A. Ted, C.R. Bass, B. Morrison 3rd, A.S. Cohen, D.F. Meaney, Primary blast injury causes cognitive impairments and hippocampal circuit alterations, Exp. Neurol. 283 (Pt A) (2016) 16–28.
[16] L.E. Goldstein, A.M. Fisher, C.A. Tagge, X.L. Zhang, L. Velisek, J.A. Sullivan, C. Upreti, J.M. Kracht, M. Ericsson, M.W. Wojnarowicz, C.J. Goletiani, G.M. Maglakelidze, N. Casey, J.A. Moncaster, O. Minaeva, R.D. Moir, C.J. Nowinski, R.A. Stern, R.C. Cantu, J. Geiling, J.K. Blusztajn, B.L. Wolozin, T. Ikezu, T.D. Stein, A.E. Budson, N.W. Kowall, D. Chargin, A. Sharon, S. Saman, G.F. Hall, W.C. Moss, R.O. Cleveland, R.E. Tanzi, P.K. Stanton, A.C. McKee, Chronic traumatic encephalopathy in blast-exposed military veterans and a blast neurotrauma mouse model, Sci. Transl. Med. 4 (134) (2012) (134ra60).
[17] V.S. Sajja, E.S. Ereifej, P.J. VandeVord, Hippocampal vulnerability and subacute response following varied blast magnitudes, Neurosci. Lett. 570 (2014) 33–37.
[18] R.K. Rowe, J.L. Harrison, T.C. Thomas, J.R. Pauly, P.D. Adelson, J. Lifshitz, Using anesthetics and analgesics in experimental traumatic brain injury, Lab. Anim. (N. Y.) 42 (8) (2013) 286–291.
[19] K.D. Statler, H. Alexander, V. Vagni, C.E. Dixon, R.S. Clark, L. Jenkins, P.M. Kochanek, Comparison of seven anesthetic agents on outcome after experimental traumatic brain injury in adult, male rats, J. Neurotrauma 23 (1) (2006) 97–108.
[20] D.H. Smith, K. Okiyama, T.A. Gennarelli, T.K. McIntosh, Magnesium and ketamine attenuate cognitive dysfunction following experimental brain injury, Neurosci. Lett. 157 (2) (1993) 211–214.

[21] G. Kannan, S.P. Kambhampati, S.R. Kudchadkar, Effect of anesthetics on microglial activation and nanoparticle uptake: implications for drug delivery in traumatic brain injury, J. Control. Release 263 (2017) 192–199.
[22] X. Lei, Q. Guo, J. Zhang, Mechanistic insights into neurotoxicity induced by anesthetics in the developing brain, Int. J. Mol. Sci. 13 (6) (2012) 6772–6799.
[23] Y. Wang, Y. Wei, S. Oguntayo, W. Wilkins, P. Arun, M. Valiyaveettil, J. Song, J.B. Long, M.P. Nambiar, Tightly coupled repetitive blast-induced traumatic brain injury: development and characterization in mice, J. Neurotrauma 28 (10) (2011) 2171–2183.
[24] M.A. Gama Sosa, R. De Gasperi, P.L. Janssen, F.J. Yuk, P.C. Anazodo, P.E. Pricop, A.J. Paulino, B. Wicinski, M.C. Shaughness, E. Maudlin-Jeronimo, A.A. Hall, D.L. Dickstein, R.M. McCarron, M. Chavko, P.R. Hof, S.T. Ahlers, G.A. Elder, Selective vulnerability of the cerebral vasculature to blast injury in a rat model of mild traumatic brain injury, Acta Neuropathol. Commun. 2 (2014) 67.
[25] R. Kuehn, P.F. Simard, I. Driscoll, K. Keledjian, S. Ivanova, C. Tosun, A. Williams, G. Bochicchio, V. Gerzanich, J.M. Simard, Rodent model of direct cranial blast injury, J. Neurotrauma 28 (10) (2011) 2155–2169.
[26] A.N. Bolton, K.E. Saatman, Regional neurodegeneration and gliosis are amplified by mild traumatic brain injury repeated at 24-hour intervals, J. Neuropathol. Exp. Neurol. 73 (10) (2014) 933–947.
[27] K.B.J. Franklin, G. Paxinos, The Mouse Brain in Stereotaxic Coordinates, Compact, 3rd ed., Elsevier, 2008, p. 256.
[28] J. Middeldorp, E.M. Hol, GFAP in health and disease, Prog. Neurobiol. 93 (3) (2011) 421–443.
[29] S. Brahmachari, Y.K. Fung, K. Pahan, Induction of glial fibrillary acidic protein expression in astrocytes by nitric oxide, J. Neurosci. 26 (18) (2006) 4930–4939.
[30] L. Wang, T.L. Hagemann, H. Kalwa, T. Michel, A. Messing, M.B. Feany, Nitric oxide mediates glial-induced neurodegeneration in Alexander disease, Nat. Commun. 6 (2015) 8966.
[31] M.T. Huuskonen, Q.Z. Tuo, S. Loppi, H. Dhungana, P. Korhonen, L.E. McInnes, P.S. Donnelly, A. Grubman, S. Wojciechowski, K. Lejavova, Y. Pomeshchik, L. Periviita, L. Kosonen, M. Giordano, F.R. Walker, R. Liu, A.I. Bush, J. Koistinaho, T. Malm, A.R. White, P. Lei, K.M. Kanninen, The copper bis(thiosemicarbazone) complex CuII(atsm) is protective against cerebral ischemia through modulation of the inflammatory milieu, Neurotherapeutics 14 (2) (2017) 519–532.
[32] S. Jinno, F. Fleischer, S. Eckel, V. Schmidt, T. Kosaka, Spatial arrangement of microglia in the mouse hippocampus: a stereological study in comparison with astrocytes, Glia 55 (13) (2007) 1334–1347.
[33] H. Dvorak-Carbone, E.M. Schuman, Patterned activity in stratum lacunosum moleculare inhibits CA1 pyramidal neuron firing, J. Neurophysiol. 82 (6) (1999) 3213–3222.
[34] M. Shimada, N. Akagi, H. Goto, H. Watanabe, M. Nakanishi, Y. Hirose, M. Watanabe, Microvessel and astroglial cell densities in the mouse hippocampus, J. Anat. 180 (Pt 1) (1992) 89–95.
[35] H. Lund-Andersen, Transport of glucose from blood to brain, Physiol. Rev. 59 (2) (1979) 305–352.
[36] W.M. Pardridge, Brain metabolism: a perspective from the blood-brain barrier, Physiol. Rev. 63 (4) (1983) 1481–1535.
[37] X. Zhao, A. Ahram, R.F. Berman, J.P. Muizelaar, B.G. Lyeth, Early loss of astrocytes after experimental traumatic brain injury, Glia 44 (2) (2003) 140–152.
[38] T.W. McAllister, Neurobiological consequences of traumatic brain injury, Dialogues Clin. Neurosci. 13 (3) (2011) 287–300.
[39] L. Amaducci, K.I. Forno, L.F. Eng, Glial fibrillary acidic protein in cryogenic lesions of the rat brain, Neurosci. Lett. 21 (1) (1981) 27–32.
[40] C. Armstrong, J. Szabadics, G. Tamas, I. Soltesz, Neurogliaform cells in the molecular layer of the dentate gyrus as feed-forward gamma-aminobutyric acidergic modulators of entorhinal-hippocampal interplay, J. Comp. Neurol. 519 (8) (2011) 1476–1491.
[41] D.G. Amaral, H.E. Scharfman, P. Lavenex, The dentate gyrus: fundamental neuroanatomical organization (dentate gyrus for dummies), Prog. Brain Res. 163 (2007) 3–22.
[42] J.V. Perederiy, G.L. Westbrook, Structural plasticity in the dentate gyrus- revisiting a classic injury model, Front Neural Circuits 7 (2013) 17.
[43] E. Forster, S. Zhao, M. Frotscher, Laminating the hippocampus, Nat. Rev. Neurosci. 7 (4) (2006) 259–267.
[44] Y. Tang, W. Le, Differential roles of M1 and M2 microglia in neurodegenerative diseases, Mol. Neurobiol. 53 (2) (2016) 1181–11984.
[45] D. Schenk, R. Barbour, W. Dunn, G. Gordon, H. Grajeda, T. Guido, K. Hu, J. Huang, K. Johnson-Wood, K. Khan, D. Kholodenko, M. Lee, Z. Liao, I. Lieberburg, R. Motter, L. Mutter, F. Soriano, G. Shopp, N. Vasquez, C. Vandevert, S. Walker, M. Wogulis, T. Yednock, D. Games, P. Seubert, Immunization with amyloid-beta attenuates Alzheimer-disease-like pathology in the PDAPP mouse, Nature 400 (6740) (1999) 173–177.
[46] K.R. Walker, G. Tesco, Molecular mechanisms of cognitive dysfunction following traumatic brain injury, Front Aging Neurosci. 5 (2013) 1–25.
[47] C. Van Den Heuvel, E. Thornton, R. Vink, Traumatic brain injury and Alzheimer's disease: a review, Prog. Brain Res. 161 (2007) 303–316.